Precision Engineering 64 (2020) 20–33

Contents lists available at ScienceDirect

Precision Engineering

journal homepage: http://www.elsevier.com/locate/precision

Abrasive flow machining (AFM) finishing of conformal cooling channels created by selective laser melting (SLM)

Sangil Han [a,*], Ferdinando Salvatore [a], Joël Rech [a], Julien Bajolet [b]

[a] Université de Lyon, ENISE, LTDS, UMR CNRS 5513, 58 Rue Jean Parot, 42023, Saint-Étienne, France
[b] IPC, Centre Technique d'Innovation en Plasturgie, 2 rue Pierre et Marie Curie, 01100, Bellignat, France

ARTICLE INFO

Keywords:
Conformal cooling channel
Selective laser melting (SLM)
Abrasive flow machining (AFM)
Straight/helical and single/multiple channels
Areal roughness parameters

ABSTRACT

Conformal cooling channels are widely adopted in the mold industry because of rapid and uniform cooling during injection molding. These complicated cooling channel geometries become feasible via selective laser melting (SLM) technology. However, the SLM fabricated internal channel surface shows high surface roughness of about 10 μm Ra. This rough surface can cause stress concentration, reducing the fatigue life of the mold. Therefore, the objective of this study is to investigate the surface finish of the SLM fabricated conformal channels by abrasive flow machining (AFM), which is widely used in the surface finishing of internal channels. To fulfill this objective, a combination of single/multiple and straight/helical channels for conformal cooling channel geometries are employed. Seven different types of conformal cooling channels (ø3mm) inside the bar are fabricated using SLM. The bar is put in the AFM fixture, and the internal channels are polished by flowing AFM media (ULV50%-54) through the channel at the same extrusion pressure of 80 bars for ten cycles. Fourteen bars (seven before AFM and seven after AFM) are machined to have the internal channel surfaces exposed for surface roughness measurement. Surface topographies of the exposed surfaces of seven types of internal channels are obtained using focus variation microscopy. The areal roughness parameters, such as arithmetical mean height (Sa) on the internal channel surfaces before and after AFM. By comparing SLM as-built conformal channel surfaces with AFM finished ones, AFM is shown to be effective in improving all SLM conformal cooling channels' arithmetical mean height, Sa. Areal roughness parameters, such as developed interfacial area ratio (Sdr), root mean square gradient (Sdq), reduced peak height (Spk), reduced valley height (Svk), and skewness (Ssk), on those internal surfaces, were found to be sensitive to surface finishing by AFM.

1. Introduction

The conformal cooling channel has been developed to have a uniform distance between the cooling channel and the part surface and to achieve a uniform and rapid cooling. Sachs et al. [1] showed that conformal cooling channels can achieve higher cooling efficiency. Dimla et al. [2] stated that a reduction in cooling time in the cycle time of the injection molding can increase productivity. The conformal cooling channels have uniform distances from the parts' surface in the mold. Thus, the rapid and uniform cooling of the conformal cooling channels can lead to higher productivity [3] and better surface quality [4] in the injection molding. Thus, conformal cooling channels are widely used in the molding industry. The conformal cooling channels are often composed of straight and round channels. They can split into multi-channels inside the mold. Fig. 1 shows an SLM fabricated mold having a conformal cooling channel. However, an SLM fabricated channel surface has high surface roughness and defects, such as partially melted powder as shown in Fig. 2. Those rough and defective surfaces can cause stress concentration during service of the molds by their repeating expansion and contraction during heating and cooling of the mold. They are detrimental to the fatigue life of the mold. Therefore, **their surface improvement by removing those defects and polishing their rough surfaces has been made by various post-processes**, such as bead-blasting [5], ultrasonic cavitation abrasive finishing [6], laser polishing [7], chemical polishing [8], and electrochemical polishing [9].

As can be seen in post-treatments on SLM surfaces, **most of the post-treatments were performed on their external surfaces.** However, to improve the surface roughness of the internal channel, special types of equipment to allow abrasives to interact with the internal surfaces were

* Corresponding author.
E-mail address: sangil.han@enise.fr (S. Han).

https://doi.org/10.1016/j.precisioneng.2020.03.006
Received 3 September 2019; Received in revised form 3 February 2020; Accepted 10 March 2020
Available online 13 March 2020

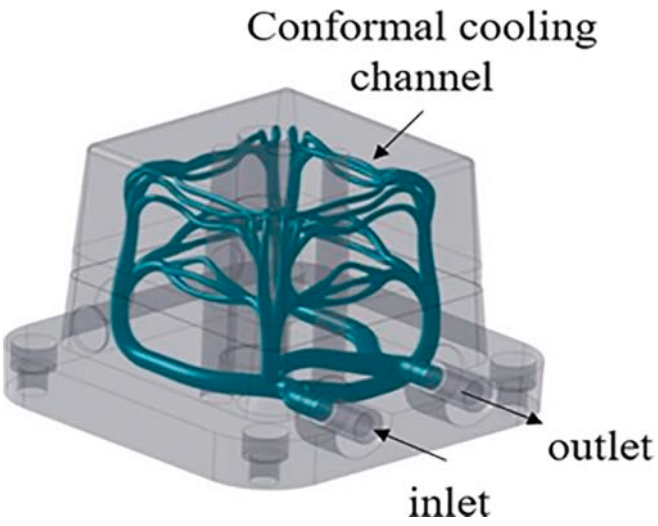

Fig. 1. A mold having a conformal cooling channel (Courtesy of IPC).

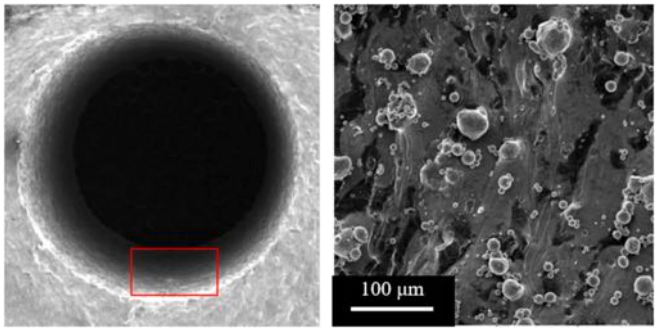

Fig. 2. SLM vertically built maraging steel 300 channel (ø3) and its surface topography.

used.

Furumoto et al. [10] fabricated a U-shaped cooling channel with a length of 80 mm and a diameter of 3 mm using SLM. They used a powder mixture consisting of alloy steel, copper, and nickel for SLM fabrication. The cooling channel is connected to two hydraulic pumps. Then, Al_2O_3 abrasive grains having a diameter of 300 μm were injected by water at a pressure of 1.4 MPa. Spiral prism-shaped microtextures, which are called protuberances, were added during SLM fabrication. The texture of the protuberances induces spiral water flow through the internal channel, leading to higher surface improvement of the internal channel. After the surface finishing of the internal channel for 2000 s, surface roughness in the channel without a protuberance decreased from 160 to 100 μm Rz while surface roughness in the channel with a protuberance decreased from 160 to 60 μm Rz. They [11] also found a significant decrease from 110 to 30 μm Rz after its surface finishing for 1000 s. Its surface roughness reached 10 μm Rz after surface finishing for 8000 s. Zhang et al. [12] input SiC (silicon carbide) or diamond slurry in an SS316 pipe having an internal diameter of 11 mm and length of 100 mm. A neodymium 52 MGOe magnetic sphere was placed inside the pipe, and neodymium 52 MGOe magnetic bars were placed near the pipe. Both the pipe and magnetic bars rotated, driving the magnetic force between the magnetic bar and sphere. The abrasives in the pipe flow through the internal pipe surface, polishing its surface. After polishing for 60 min, its surface roughness in 2-mm-long regions in the pipe decreased from 4.165 to 0.078 μm Ra. Yamaguchi et al. [13] polished internal surfaces of SUS304 stainless steel bent tube with an internal magnetic abrasive finishing process. They drove magnetic force by rotating two pairs of N–S poles around the external tube surface, allowing iron particles to flow through and polish the internal tube surface. Surface roughness in both straight and bent regions of the internal surface decreased from 3 to 0.05 μm Ra.

Abrasive flow machining (AFM) is known to be effective to finish internal channel surfaces. A schematic illustration of a two-way AFM is given in Fig. 3. The AFM media, where polymer and SiC (silicon carbide) abrasives are mixed, is filled into the lower cylinder of the AFM machine. The workpiece having an internal channel is placed on the fixture that is connected to the lower cylinder. Then, the workpiece is clamped by the upper cylinder. The AFM media flows upward and downward through the internal channel by the stroke movements of the pistons in the cylinder, as shown in Fig. 3(a)(b). One cycle is completed by the up- and down-strokes in the two-way AFM machine. The internal channel surface material is removed by interactions (e.g., ploughing, cutting) between the abrasives and the channel surface. As a result, the internal channel surface roughness improves.

Williams et al. [14] adopted the profiled edge laminae (PEL) to build conformal channels and used aluminum (6061-T6) or carbon steel (AISI 1008) as a laminae material. They performed AFM through the two channels' internal surfaces using 70-grit-size AFM media at an extrusion pressure of 6.89 or 8.96 MPa for 2 cycles. Its flow media volume was 350 $inch^3$. No leakage was observed after flowing water through those channel surfaces at a pressure ranging from 276 to 689 kPa. AFM was attributed to the effective sealing between stacked laminae. Surface roughness improvement from 4.9 to 0.13 μm Ra was observed in those internal channel surfaces. In the previous research done by Duval-Chaneac et al. [15], they created an SLM maraging steel 300 pin part. It is assembled with a 40-mm-long internal channel (ø14.5). They finished the pin part's surface with four different AFM media, with different media viscosity (low viscosity (LV) and medium viscosity (MV)) and abrasive weight concentration (35, 50, and 65%) but with the same grit size (150 grit). A significant reduction in surface roughness from 13 to 2 μm Sa after AFM with MV65%-150 having a medium viscosity (MV) and higher abrasive concentration (65%) has been observed.

In the previous attempts to finish the internal channels, such as L-shaped, U-shaped, and straight channels, the channels have a short and simple geometry. By contrast, **conformal cooling channels in molds adopt longer and more complicated channel geometries.** They form helical (spiral) and/or multi-channels to surround the part in the molds. **Thus, it is necessary to fabricate more complex shapes of conformal channels by SLM.** Then, the conformal channel surfaces are finished by AFM. Their surface roughness improvement is discussed in terms of areal surface roughness parameters.

2. Experimental methods

2.1. Selective laser melting (SLM) conformal channel fabrication

As mentioned in the introduction, conformal channels constitute different shapes of channels and multi-channels to surround the part in the injection molding. Therefore, different shapes of channels, such as straight and helical channels, were proposed in this study. Single and multiple channels were also proposed and given by varying their channel numbers from one to three. Table 1 lists conformal cooling channels having different shapes and numbers of channels to study their fabrication by selective laser melting (SLM) and finished by abrasive flow machining (AFM).

These conformal cooling channels were fabricated by selective laser melting (SLM) using an SLM machine (EOS M270). Maraging steel 300 is employed as a powder material in this study because it is widely used in the mold industry and can be applied to the mold having a conformal cooling channel. As shown in Fig. 5, different types of internal cooling channels were built in the bar by selective laser melting (SLM). The SLM is done in the vertical direction. Thus, as shown in Fig. 5(a), the straight channel has the same direction as the SLM building one. The SLM bar is

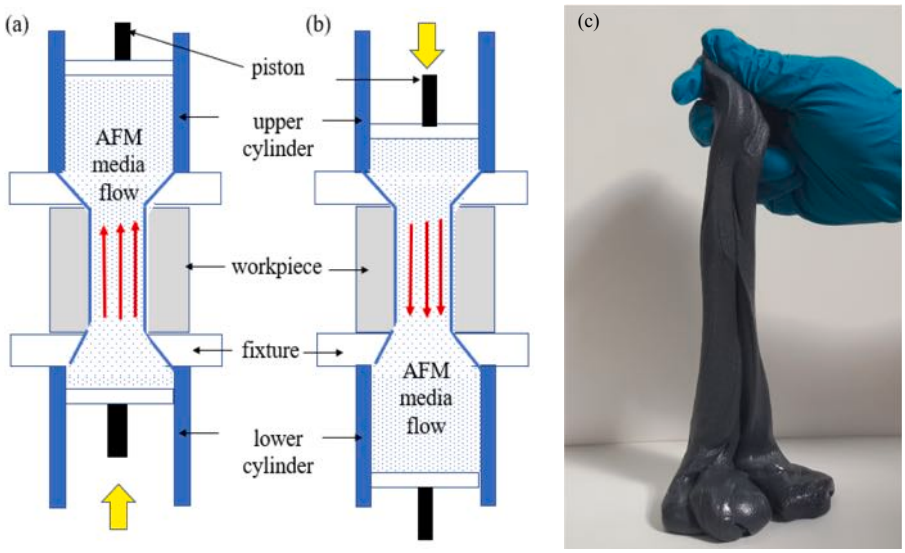

Fig. 3. A schematic illustration of a two-way AFM: (a) up-stroke, (b) down-stroke, and (c) AFM media (MV50%-150).

Table 1
Conformal cooling channels having different shapes and numbers of channels.

Channel type	Channel shape	Number of channels	Total channel length (mm)	Channel diameter (mm)	Ratio of total channel length to channel diameter (L/D)
1	Straight	1 channel	120	3	40
2	Straight	2 channels	240	3	80
3	Straight	3 channels	360	3	120
4	Helical	1 channel	240	3	80
5	Helical	2 channels	480	3	160
6	Helical	3 channels	720	3	240
7	Helical	1 channel with smaller lead	360	3	120

21 mm in diameter and 110 mm long. We chose an internal channel diameter of 3 mm so that we have a high ratio of the internal channel diameter to its channel length.

2.1.1. Geometric characteristic in helical channels

The helical channel is characterized by a helix. Trigonometry to characterize lead and lead angle in a helical channel (type #4) is shown in Fig. 6.

A conformal channel (type #4) has a lead of $l_{lead} = 21.9$ mm and a lead angle of $\theta = 27.8°$. The channel center forms a helix with a diameter of $d_r = 13.2$ mm. Table 2 compares dimensions in helical channels between type #4 and #7.

Table 2 shows that a helical channel (type #7) has a smaller lead than that of type #4. Thus, it has a longer channel length (360 mm) than that (240 mm) of the channel (type #4). All types of conformal channels from type #1 to #7 were finished with AFM.

2.2. AFM finishing of conformal cooling channel

We designed an AFM fixture to hold the SLM bar and to flow AFM media through the conformal channel for its surface finishing. The experimental set up for AFM finishing of the conformal channel surface and its cross-section view are shown in Fig. 7. A two-way AFM machine (Extrude Hone) is employed to perform AFM on the conformal cooling channel as shown in Fig. 7(a). Cross-section views of the SLM bar and its AFM fixture are given in Figs. 7(b) and Fig. 8. The SLM samples have the same inlet and outlet to flow AFM media as shown in Fig. 4. Two caps were covered over the top and bottom surface of the SLM bar, and then they were placed into the sleeve. All elements, such as the SLM sample, two caps, and the sleeve were fixed at the top and bottom regions. Then, they were mounted on the AFM fixture and clamped by lowering the upper AFM cylinder. By applying AFM pressure with upper and lower cylinders in the AFM machine, AFM media flows through the internal cooling channel in the SLM bar. Parameters of the AFM media and the AFM machine are given in Table 3.

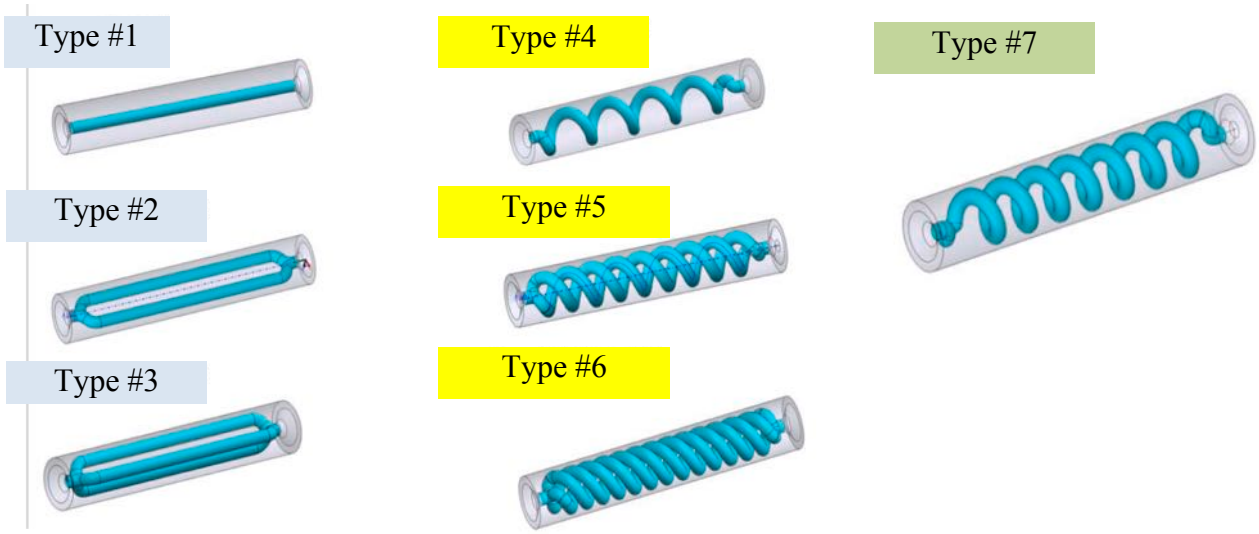

Fig. 4. CAD modeling of bars having seven types of conformal cooling channels (ø3mm): from type #1 to #7.

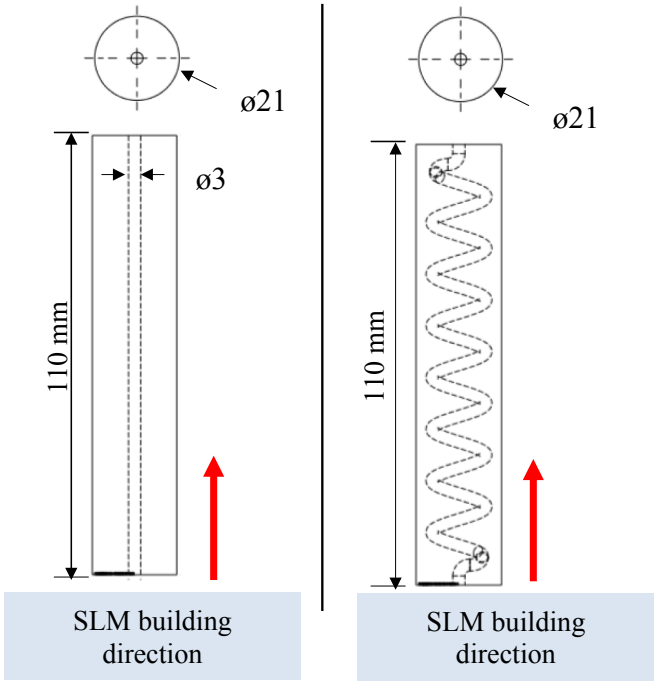

Fig. 5. SLM bar and conformal channel fabrication: (a) one straight channel (type #1), (b) one helical channel (type #7).

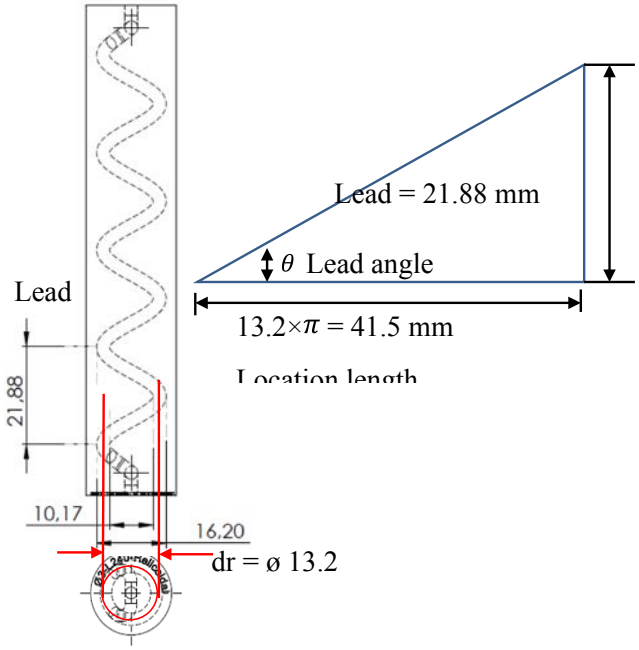

Fig. 6. Trigonometry to characterize lead and lead angle in a helical channel (type #4).

AFM media, ULV50%-54, is used. Silicon carbide (SiC) abrasive and polyboroxane polymer carrier were used in the AFM media. It stands for ultra-low viscosity, abrasive concentration (wt. %) of 50%, and abrasive grit size of 54. AFM media with ultra-low viscosity (ULV) is chosen because it is effective to polish a small diameter channel (ø3) as compared to the workpiece channel (ø14.5) in the previous study [15]. The extrusion pressure by the AFM cylinder was set to be 80 bars (8 MPa). The flow volume per each stroke of AFM, that is, up-stroke and down-stroke of the AFM flow, was set to be 327741 mm^3. Since one cycle of two-way AFM is composed of one up-stroke and one down-stroke, the flow volume per one cycle is 655482 mm^3. AFM finishing of each type of conformal channel surface was performed for 10 cycles.

Table 2
Dimensions in helical channels (type #4 and #7).

Channel type	Lead (mm)	Channel center path diameter (mm)	Location length (mm)	Lead angle (degree)
Type #4	21.88	13.2	41.5	27.8
Type #7	13.07	13.2	41.5	17.5

2.3. AFM flow characterization — velocity of AFM media flow

We employed seven types of conformal channels, which differ in the number of channels and the total channel length as given in Table 1. We characterized AFM flow in terms of velocity of AFM media flow. To calculate the velocity of AFM media flow, a diagram to show AFM media

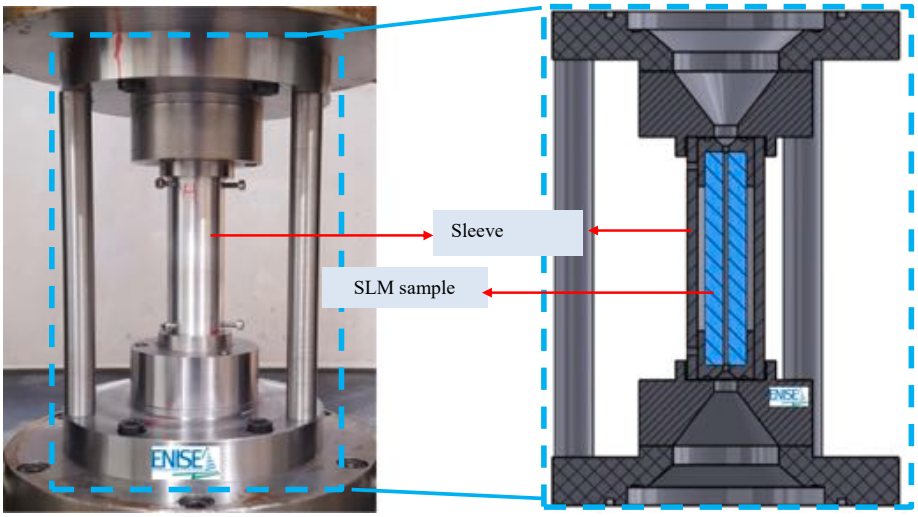

Fig. 7. (a) Experimental set up for AFM finishing of the conformal channel surface and (b) a cross-section view of the SLM bar (type #1) and its AFM fixture.

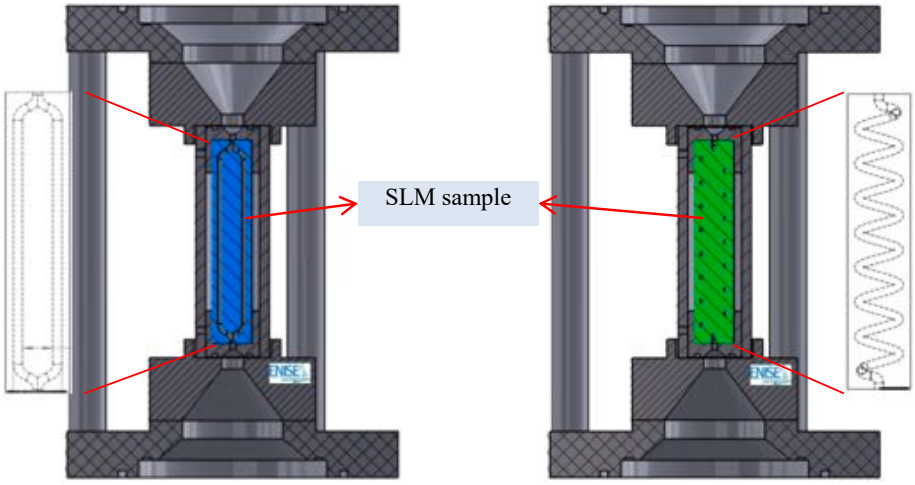

Fig. 8. Cross-section views: (a) SLM bar (type #2) and (b) SLM bar (type #7) and its AFM fixture. Hidden lines are shown in each SLM bar.

Table 3
AFM parameters used in AFM finishing.

AFM media	ULV50%-54
Extrusion pressure (bars)	80
Flow volume per one cycle (inch^3)	40 (0.66 L)
Cycle	10

flow in single and multiple channels is given in Fig. 9.

As specified in Table 3, the flow volume of AFM media per one cycle, $V_{cylinder}$, is 655482 mm^3. We measure one cycle time, t_{cycle} (sec), during AFM. Thus, the flow rate, $Q_{cylinder}$ (mm^3/sec), through the cylinder of the AFM machine can be expressed as (1)

$$Q_{cylinder} = \frac{V_{cylinder}(mm3)}{t_{cycle}(sec)} \quad (1)$$

Jain et al. [16] used a continuity equation to calculate the velocity of AFM media flow through the channel. In Fig. 9(a), using the continuity equation, $Q_{cylinder}$ can be given as (2) in terms of the average velocity of AFM media flow through the AFM cylinder, v_1, and the average velocity of AFM media flow through the conformal channel, v_2. A_2 is a cross-section area (mm^2) in the conformal channel, thus, $A_2 = \pi \times \left(\frac{d}{2}\right)^2 = \pi \times \left(\frac{3\text{ mm}}{2}\right)^2 = 7.1\text{ mm}^2$.

$$Q_{cylinder} = A_1 \times v_1 = A_2 \times v_2 \quad (2)$$

The average velocity of AFM media flow in one channel, v_2 (mm/sec), in Fig. 9(a), can be given by

$$v_2 = \frac{Q_{cylinder}}{A_2} = \frac{V_{cylinder}\ (mm3)}{t_{cycle}(sec) \times A_2(mm2)} \quad (3)$$

In the case of AFM flow through two channels in Fig. 9(b), using the continuity equation, $Q_{cylinder}$ can be given as (4) in terms of the average velocity of AFM media flow through the AFM cylinder, v_1, and the average velocity of AFM media flow through the conformal channel, v_3.

$$Q_{cylinder} = A_1 \times v_1 = A_3 \times v_3 = 2 \times A_2 \times v_3 \quad (4)$$

Thus, the average velocity of AFM media flow through two channels, v_3 (mm/sec), in Fig. 9(b) can be given by

$$v_3 = \frac{Q_{cylinder}}{2 \times A_2} = \frac{V_{cylinder}\ (mm3)}{t_{cycle}(\text{sec}) \times 2 \times A_2(mm2)} \quad (5)$$

In the case of AFM flow through three channels in Fig. 9(c), using the continuity equation, $Q_{cylinder}$ can be given as (6) in terms of the average velocity of AFM media flow through the AFM cylinder, v_1, and the

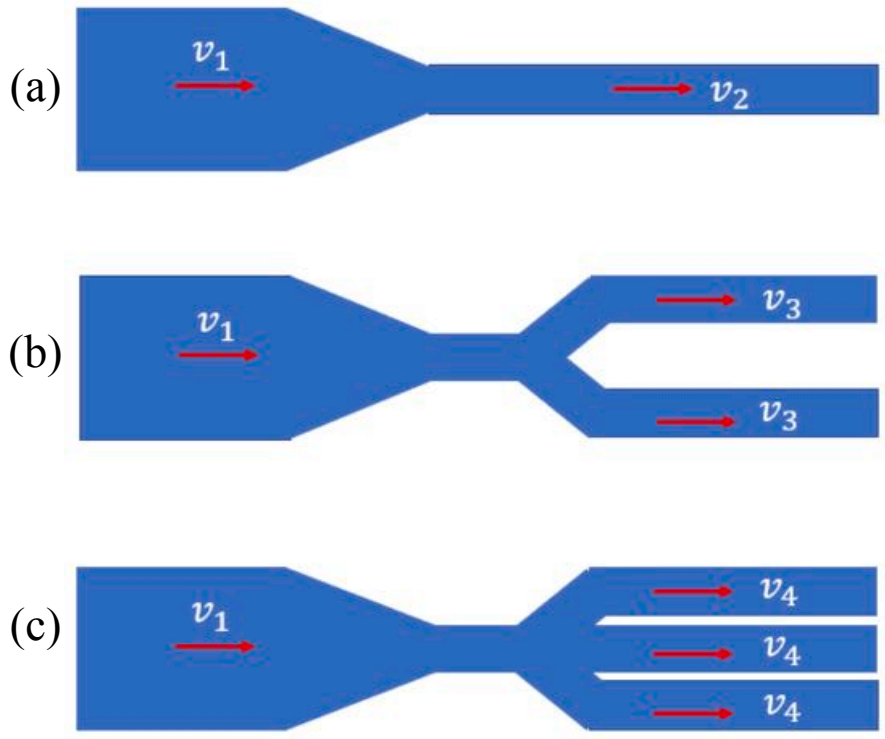

Fig. 9. Velocity of AFM media flow in: (a) 1-channel, (b) 2-channel, (c) 3- channel.

average velocity of AFM media flow through the conformal channel, v_4.

$$Q_{cylinder} = A_1 \times v_1 = A_4 \times v_4 = 3 \times A_2 \times v_4 \quad (6)$$

Thus, the average velocity of AFM media flow in three channels, v_4 (mm/sec), in Fig. 9(c) can be given by

$$v_4 = \frac{Q_{cylinder}}{3 \times A_2} = \frac{V_{cylinder}\ (mm3)}{t_{cycle}(\text{sec}) \times 3 \times A_2(mm2)} \quad (7)$$

We measured a total cycle time in AFM for 10 cycles. The total cycle time in AFM for 10 cycles is given in Fig. 10. A cycle time, t_{cycle}, can be calculated by dividing the total cycle time by 10. The average velocities of AFM media flow, such as v_2, v_3, and v_4 through one, two and three channels can be calculated using Eq. (3), Eq. (5), and Eq. (7), respectively.

The average velocities of AFM media flow in all types of conformal channels are given in Fig. 11. The velocity of AFM media flow in the straight conformal channels (type #1, #2 and #3) decreases as the number of channels increases. The velocities of AFM flow in two and three straight channels are 27% and 45% lower than that in one straight channel. The same trend is seen in the helical conformal channels (type #4, #5, and #6). The velocities of AFM flow in two and three helical channels are 47% and 66% lower than that in one helical channel. The average velocity of AFM media flow decreases as the total channel length increases among type #1, #4, and #7 having one channel. The velocities of AFM flow in one helical channel with big and small lead angle are 26% and 46% lower than that in one straight channel. This observation can be due to the bigger minor loss, which results from the bigger friction between the AFM media and the surface in the longer channel.

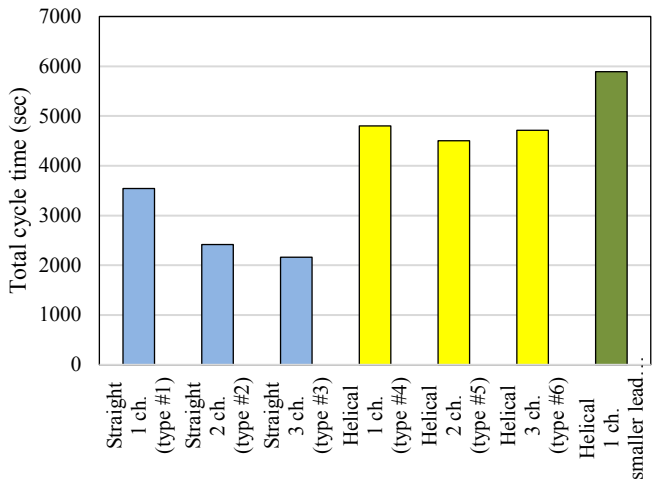

Fig. 10. Total cycle time in AFM for 10 cycles of conformal cooling channels.

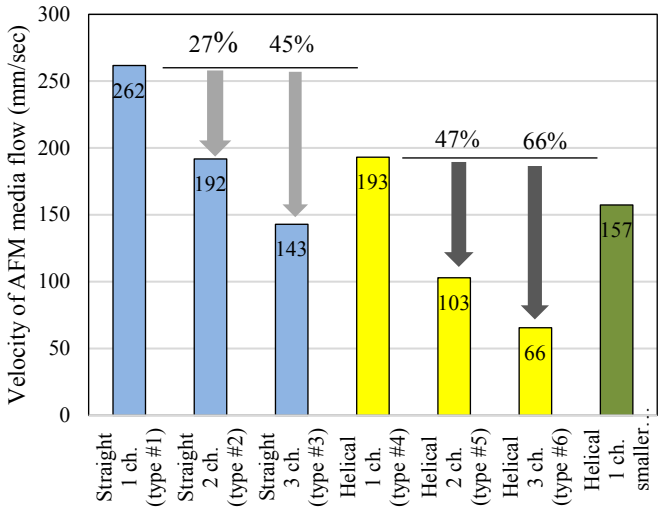

Fig. 11. The average velocity of AFM media flow in each type of channel.

2.4. Characterization of the surface topography of the conformal cooling channels

To compare the surface topography of all types of conformal channels before and after AFM, we characterize the surfaces of conformal channels with a focus variation microscopy. Surface roughness measurement of different types of internal channels using a contact stylus is constrained to their internal channel geometries. Thus, to measure surface roughness of those conformal cooling channels, we machined the SLM bar by milling (type #1) and grooving (type #2 to #7) in a CNC milling and turning machine. Those internal surfaces were exposed. Then, we used a focus variation microscope (InfiniteFocus G5, Alicona) to measure surface roughness of the exposed internal channel surface before and after AFM finishing. The dimension and pictures of the machined region of SLM bars are given in Fig. 12 and Fig. 13.

The grooved SLM bar was mounted on the stage of the focus variation microscope as shown in Fig. 14. As indicated as a rectangular region on each grooved SLM bar in Fig. 13, the measured areas are (2.5 × 3) mm for channels. The measurement was conducted with a 20× objective lens with a vertical resolution of 50 nm and a lateral resolution of 2 μm. The pixel size is (0.438 × 0.438) μm. Three different points in each type of conformal channel were measured.

We analyzed the internal channel surface (type #3) using scanning with the focus variation microscopy. The internal channel surface is given as a height map in Fig. 15(a). The internal channel surface is cylindrical in shape, as shown in Fig. 15(a). The cylindrical form is removed by the form removal process using the software (Alicona), as shown in Fig. 15(b). The "form removal" process of the helical channel surface (type #7) is shown in Fig. 16. Even after the cylindrical surface, with its channel diameter of $d_{channel} = 3$ mm, is removed, there is still a cylindrical surface with a helix diameter of $d_r = 13.2$ mm, as shown in Fig. 16(b). Thus, the form removal process is done, and the final form removed surface was obtained as shown in Fig. 16(c).

After the "form removal" process of the internal channel surface, for areal texture (ISO 25178-2) analysis of its surface, we select a rectangular region of (2 × 2) mm on the surface. Thus, after the "form removal" process twice, we rotate the "form removed" surface by 62° with respect to the Z-axis using the software (Alicona). After rotating it, we chose a (2 × 2) mm region as shown in Fig. 17. To analyze areal texture parameters, we applied a cutoff wavelength of Lc = 0.8 mm in both X and Y directions on the chosen (2 × 2) mm region in Fig. 17. Then, we used a "Gaussian filter for flat surfaces" (ISO 16610-61, Linear Planar, Order 0).

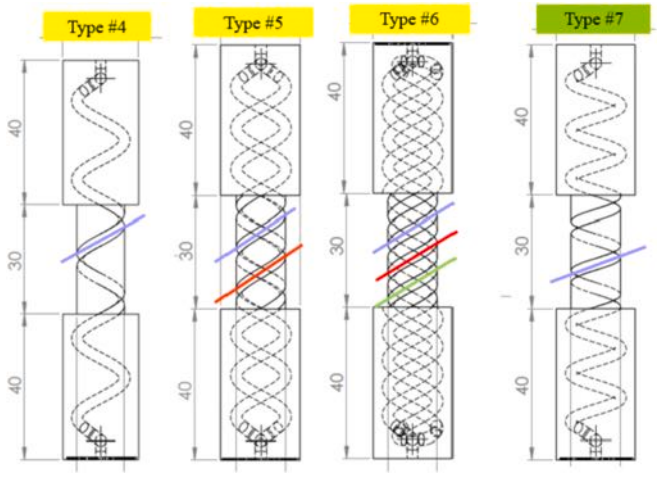

Fig. 12. Dimensions of SLM bars where internal channels were exposed after grooving (type #4 to #7).

3. Results and discussion

3.1. Optical micrographs of the surface of conformal cooling channels before and after AFM

Optical micrographs and corresponding color height maps before and after AFM are given in Fig. 19 for straight channels and in Fig. 20 for helical channels. The channel direction of the straight conformal cooling channels (type #1, #2, and #3) corresponds to the SLM building direction. We recall that the SLM bars were fabricated at a building angle of 90°, as shown in Fig. 5. These straight conformal channel surfaces in Fig. 19(a) correspond to the side surfaces of the SLM built channel. After performing AFM for 10 cycles in the straight conformal channels, AFM flow marks are visible on their surfaces in Fig. 18(b). These optical micrographs reveal a significant surface topography change by AFM.

As shown in Fig. 18(a), the channel direction of the helical conformal cooling channels (type #4, #5, and #6) is indicated as a white arrow. The SLM building direction is indicated as a red arrow. The channel direction and the SLM building direction form a 62° angle, as shown in Fig. 17. This is a complementary angle of the lead angle of $\theta = 28°$, as given in Table 2. The AFM flow direction is indicated as a yellow arrow in Fig. 18(b). AFM flow marks are also quite visible. The SLM surface texture was removed. However, more valley regions in the helical channel surface (type #4) are observed than those in the straight channel surfaces (type #1, #2, and #3). The surface in the channels (type #5 and #6) appears to be rougher than other surfaces. This observation can be linked to the lower velocity (See Fig. 11) of AFM flow in the channels (type #5 and #6). It appears that the SLM surface texture in the conformal channel (type #7) was removed more than those of channels (type #5 and #6) because its velocity (See Fig. 11) of AFM flow is higher than those of channels (type #5 and #6), as shown in Fig. 11. In addition to optical micrograph analysis in this section, surface texture characterization in terms of areal parameters is conducted in the next section.

3.2. Areal parameter analysis of surfaces in conformal cooling channels

As discussed in introduction, AFM has been shown to be effective to polish internal channels [14–20]. Very low level of surface roughness by 0.4 μm Ra [17] after AFM has been achieved. It can be noted that the initial channel surface textures before AFM were produced by conventional processes, such as milling [17], turning [18]. However, SLM built surface is characterized by irregular textures, such as unmolten power, local waving, pits, and cracks [5]. Thus, areal surface roughness parameters (ISO 25178-2) have increasingly employed to characterize textures and topographies of SLM built surfaces. Therefore, characterization of the surface topography of conformal channel surfaces before and after AFM in terms of areal roughness parameters (ISO 25178-2) is mainly addressed in this section.

As shown in Figs. 15–17, we conducted a "form removal" process and chose a region on the internal surface of all types of internal channel surface (from type #1 to #7). Then, those surfaces were analyzed in terms of areal roughness parameters (ISO 25178-2). Fig. 20(a) shows arithmetical mean height, Sa, of the conformal cooling channel surfaces before and after AFM. The straight cooling channel surfaces (type #2 and #3) have arithmetical mean height of about 8 μm Sa. On the other hand, the helical cooling channel surfaces (type #4 to #7) exhibit arithmetical mean height of about 10 μm Sa. We recall the straight and helical channels in Fig. 20(b). The staircase effect is observed on the inclined surfaces fabricated layer-by-layer in SLM in Fig. 21. Thus, this staircase effect can contribute to a higher areal roughness of the helical channel surfaces than that of the straight channel.

As we compare areal roughness progress between a 1-helical channel and 2- and 3-helical channels (e.g., type #4 vs. type #5 and #6), surface roughness progress in the 2- and 3-helical channels is lower than that in the 1-helical channel. This observation can be attributed to the velocities

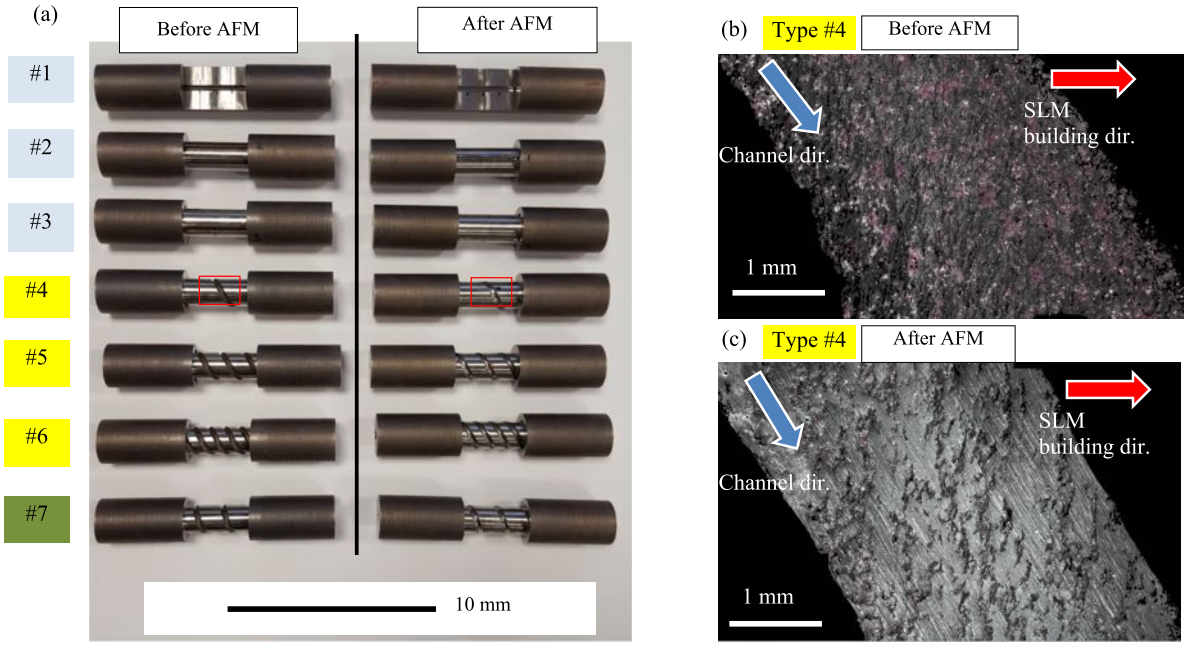

Fig. 13. Grooved SLM bars where internal channels were exposed after grooving: (a) A total of 14 bars (seven before AFM and seven after AFM) are illustrated, Optical micrographs of channel surfaces (type#4): (b) before and (c) after AFM.

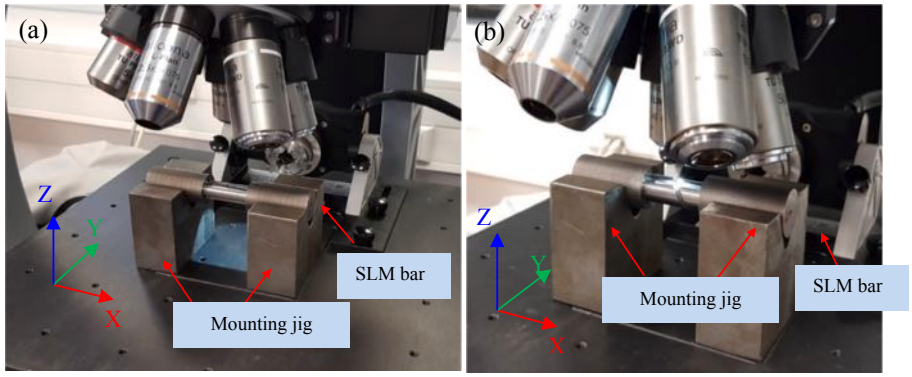

Fig. 14. SLM bars mounted on the jig on the focus variation microscope stage: (a) straight three-channel (type #3) and (b) helical one-channel (type #4) samples were exposed.

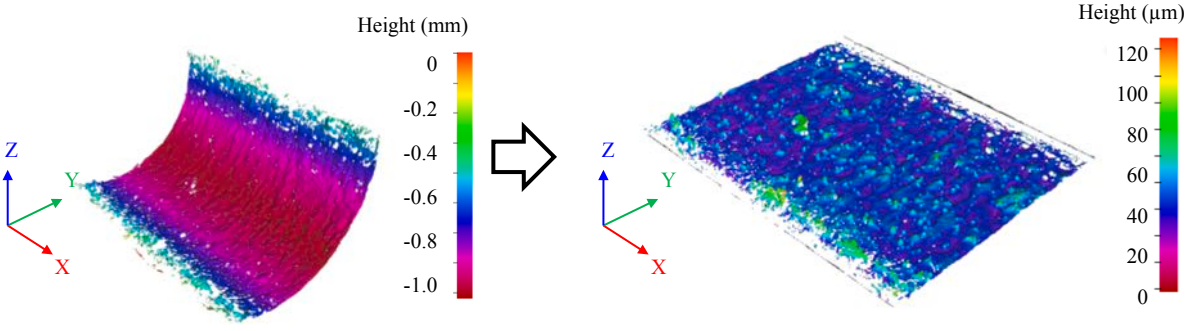

Fig. 15. "Form removal" process of the straight channel surface (type #3): (a) internal channel surface and (b) "form removed" surface.

of AFM media flow in type #5 and #6 (2- and 3-helical channels) being lower than that in the 1-helical channel (type #4), as shown in Fig. 11. In addition to the velocity of AFM media flow, less amount of AFM media passes through the multi-channel than through the single channel. Thus, less amount of abrasive grains flow on the channel surface, reducing opportunities to decrease the surface roughness. We recall the different total channel lengths such as 120, 240, and 360 mm in the single channels (e.g., type #1, #4, and #7) in Table 1. As we compare areal

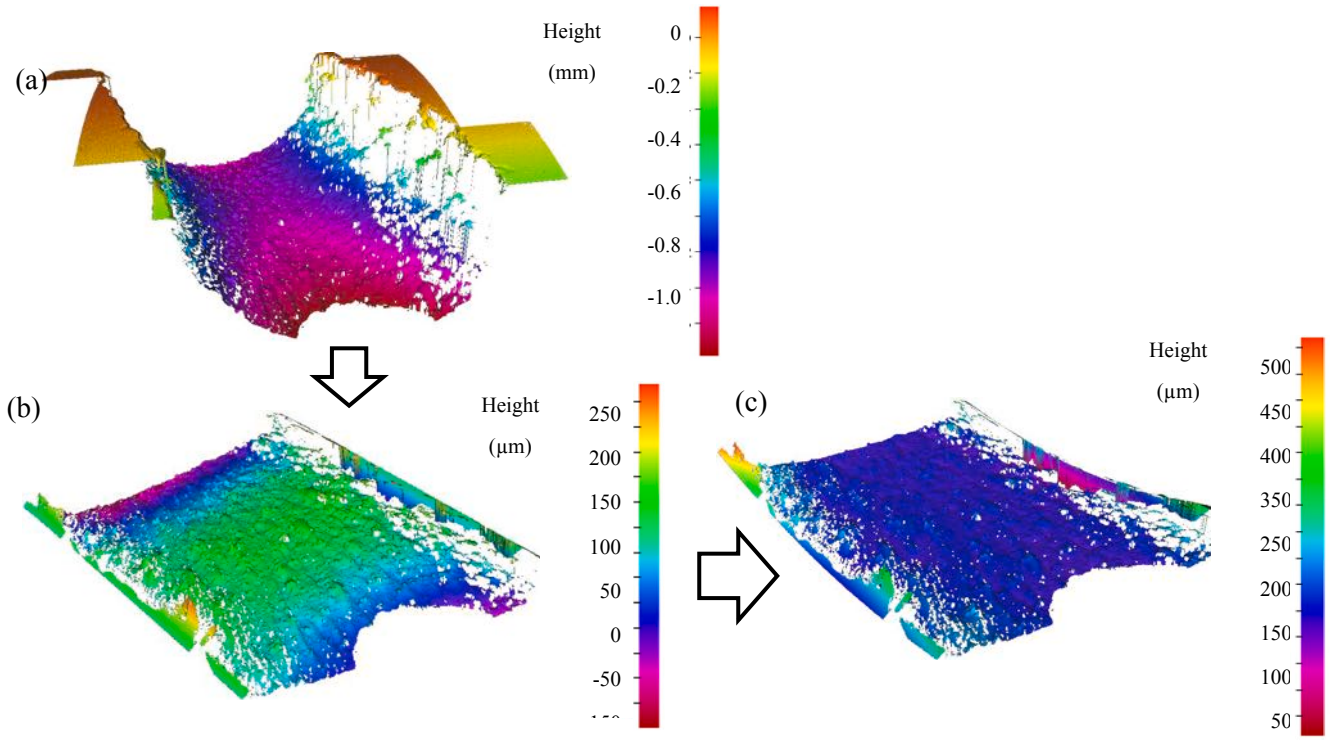

Fig. 16. "Form removal" process of the helical channel surface (type #7): (a) internal channel surface, (b) "form (cylindrical surface with a channel diameter) removed" surface, (c) "form surface (cylindrical surface with a helix diameter) removed".

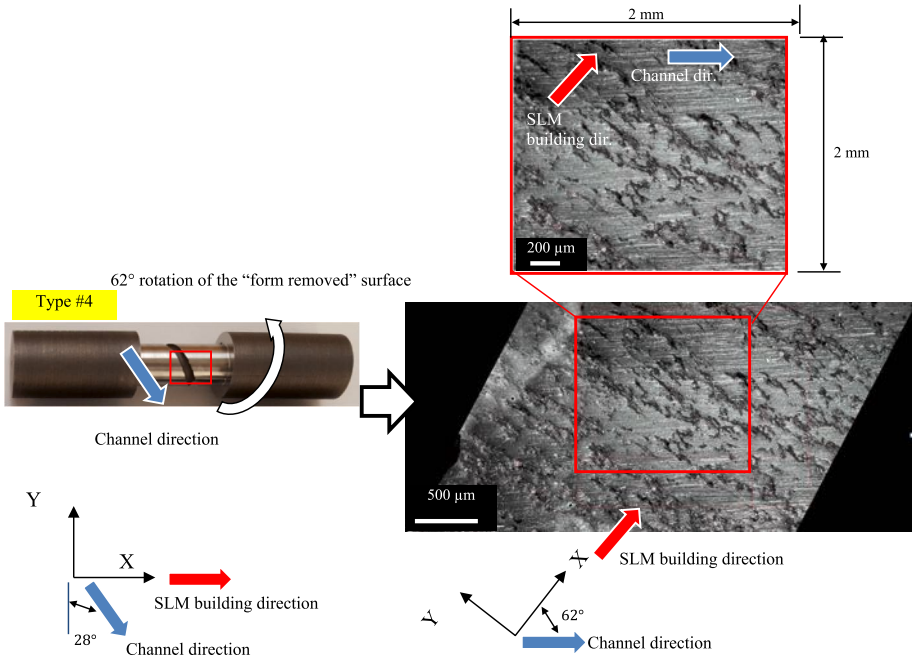

Fig. 17. Internal channel surface selection for areal texture (ISO 25178-2) analysis in the helical channel surface (type #4) after AFM. ("dir." indicates direction.)

roughness progress between single channels having different channel lengths, (type #4 vs. type #7), surface roughness progress decreases with its channel length increasing. In Fig. 11, it can be seen that the velocity of AFM media flow in the single channel (type #1, #4, and #7) decreases as its channel length increases. This observation can contribute to the difference in the areal roughness progress among samples having a single channel.

The root mean square gradient, Sdq, and the developed interfacial area ratio, Sdr, of SLM internal channel surfaces were also found to be sensitive to the AFM process. A schematic illustration of the evolution of Sdr and Sdq values of the surface is given Fig. 22. As the slope of the surface texture decreases, Sdq decreases in Fig. 22(a). The surface area of the texture also decreases. Thus, Sdr also decreases. Thus, Sdr decreases in Fig. 22(b).

The root mean square gradient, Sdq, of SLM internal channel surfaces before and after AFM is given in Fig. 23. High peak regions in the initial

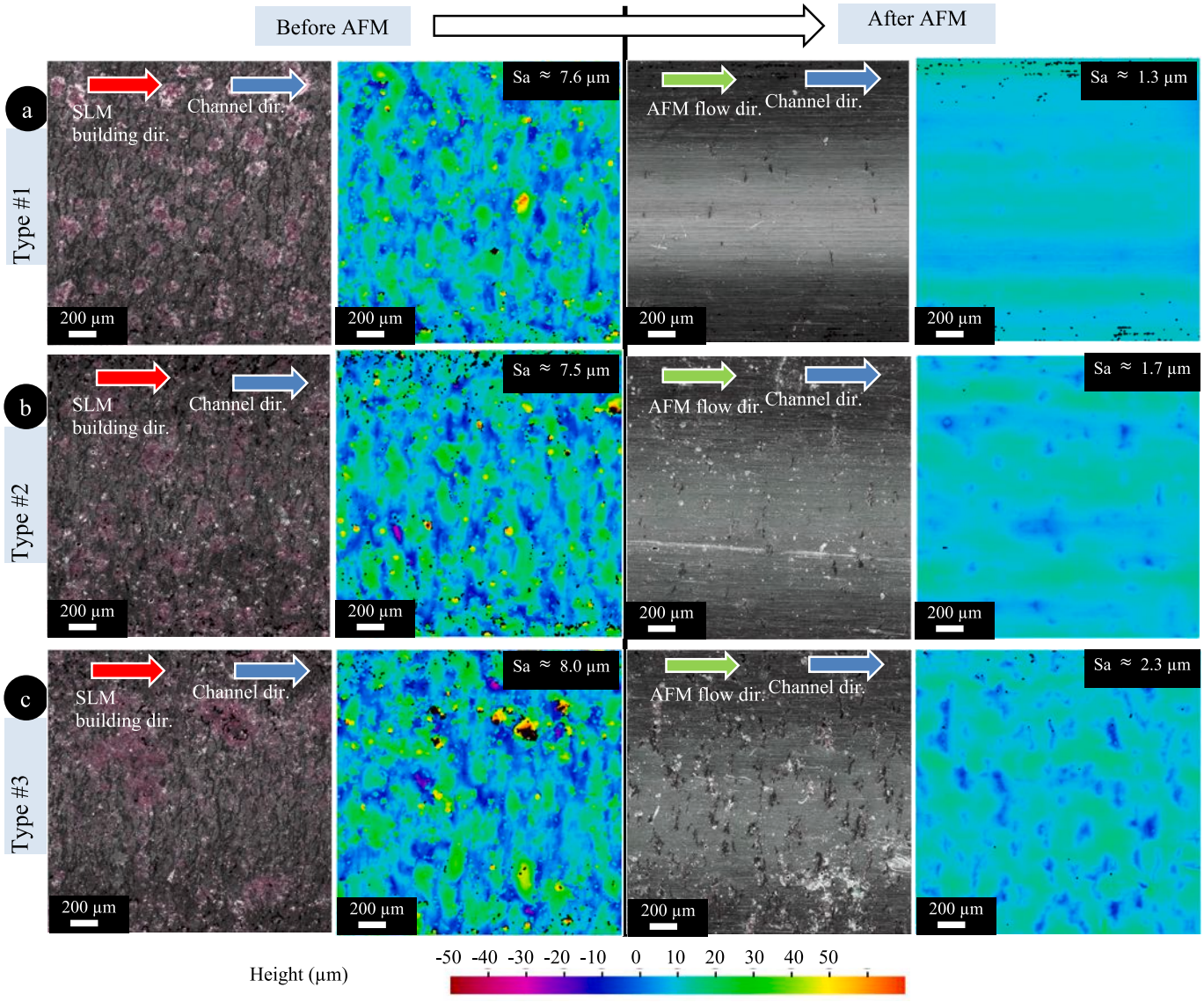

Fig. 18. Optical micrographs and height color maps of straight channels before and after AFM: (a) type #1, (b) type #2, and (c) type #3.

internal surface fabricated by SLM have a high surface gradient, resulting in higher root mean square gradient value of Sdq. They range from 0.9 to 1.2 Sdq. The SLM texture, such as peak regions of internal surfaces, were removed after AFM. Therefore, their surface gradient can change from sharp to gradual gradient after AFM.

This observation can justify that their Sdq value decreases up to 0.2 in the straight channel surfaces. In helical channels, such as type #5, #6, and #7, their Sdq values range from 0.3 to 0.4 due to their lower surface roughness progress than those of straight channels.

As shown in Fig. 24, the initial surfaces of SLM internal channels have a very high developed interfacial area ratio, from 30 to 50% Sdr. High peak regions observed in SLM fabricated internal surfaces can increase their additional surfaces, causing higher values of Sdr. After AFM for 10 cycles, their developed interfacial area ratio decreased to 2% in Sdr, indicating that their surfaces are close to a flat surface. In helical conformal cooling channels (type #5, #6, and #7), their Sdr values range from 7 to 9% due to their lower surface roughness improvement than those of straight channels (type #1, #2, and #3).

We analyzed the reduced peak height, Spk, and reduced valley height, Svk, before and after AFM. We also analyzed the skewness of the selected area. As shown in Fig. 26(a), the SLM fabricated initial surfaces of all types of channels show very high reduced peak values of about 20–30 μm Spk. Those values are much higher than those of a reduced valley of about 10 μm Svk in Fig. 26(b). Therefore, its skewness exhibits a high positive value over 1 in Fig. 27. As shown in Figs. 19 and 20, in comparison of micrographs of the internal surfaces before and after AFM, most of the peak regions were removed after AFM for 10 cycles. AFM flow lines and some remaining valley regions were observed. This surface topography evolution and areal parameters are illustrated in Fig. 25. Thus, reduced peak values after AFM decreased significantly below 5 μm Spk in the surfaces, such as type #2 to #6 as shown in Fig. 26 (a). Since some valley regions remain on their surfaces after AFM, their reduced valley values are over 5 μm Svk in Fig. 26(b). Thus, negative skewness after AFM is observed in their surfaces in Fig. 27. In the conformal channel surface (type #7), although its reduced peak value is higher than 5 μm Spk after AFM in Fig. 26(a), its reduced valley value is about 11 μm Svk after AFM in Fig. 26(b). Thus, its skewness value is also negative in Fig. 27.

In this section, surface topography of SLM built and AFM finished conformal channel surfaces was characterized by areal roughness parameters (ISO 25178-2), such as Sa, Sdr, Sdq, Spk, Svk, and Ssk. It can be noted that most of AFM works have been dedicated to investigation of Ra change after AFM finishing of the surface with regular textures produced by conventional process [1,2]. However, as mentioned earlier

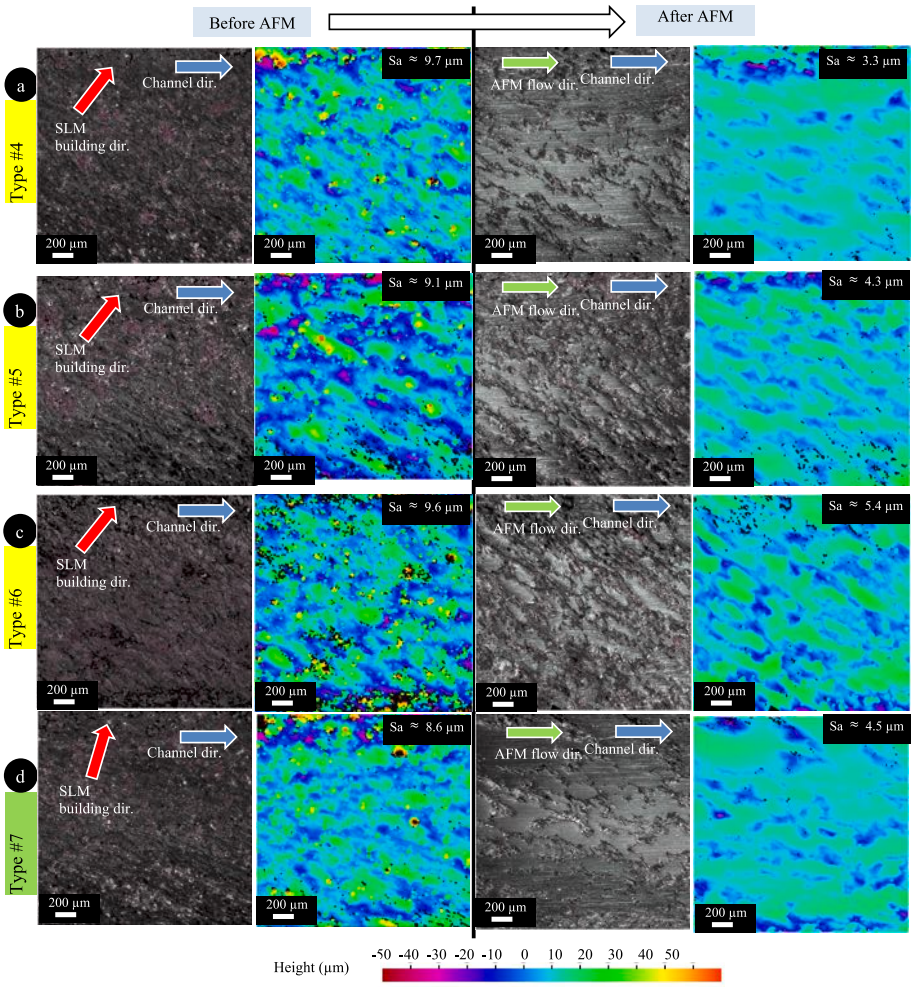

Fig. 19. Optical micrographs and height color maps of helical conformal channel surfaces before and after AFM: (a) type #4, (b) type #5, (c) type #6, and (d) type #7.

in this section, SLM built surface exhibits very irregular patterns. Surface topography characterization in this section can provide more insights on the capability of the AFM process to finish the SLM built conformal cooling channel.

3.3. *Effect of the surface roughness on the cooling performance of the channel*

The effect of the roughness on the cooling performance of the internal channel also has been studied. As compared to SLM built internal channel, the counterparts with lower surface roughness have been produced by free abrasive grains [11], drilling [21], and heat treatment [22]. Furumoto et al. [11] performed free abrasive finishing, leading to surface roughness improvement from 80 to 20 μm Rz. They found 4% reduction in cooling time in the finished surface as compared to the initial rough surface. Liu et al. [21] compared cooling performance between SLM built and drilled cooling channels. Surface roughness of the SLM built channel was much higher (Ra = 14 μm) than that of drilled channel surface (Ra = 6 μm). In their study, the cooling performance was indicated in terms of Nusselt number, Nu, and fluid flow rate. The cooling performance of the SLM built channel was shown to be lower than that of the drilled one. Snyder [22] improved the SLM Inconel-939 channel surface roughness (from 35 to 20 μm Ra) by heat treatment, which is done at temperature close to melting range for 8h. The roughness of the cooling channel can affect the heat transfer and pressure drop on its surface. They are compromising factors. In the heat treated channel surface (Ra = 20 μm), he found 50% reduction in pressure drop, while only 18% reduction in heat transfer as compared to those in SLM as built channel surface (Ra = 35 μm). Consequently, the overall cooling efficiency was found to increase in the channel surface with lower surface roughness. Previous studies show that improved surface roughness can enhance the cooling performance of the channel. Thus, AFM finished SLM built conformal cooling channel is expected to increase its cooling performance as compared to the SLM as-built one.

3.4. *AFM finished SLM built channel's surface roughness compared to conventional channel's roughness*

The AFM finished channel's surface roughness can also be compared to the practical specification of the internal cooling channel. In conventional cooling channel system, especially in the injection molding industry, drawn metal pipes, such as copper, brass, and stainless steel, are employed. Their typical internal surface roughness of new drawn copper and stainless pipes varies from 1.5 to 10 μm Rz [23]. Rz value can be used to represent the surface roughness of the pipe surface [24]. The channel surface (type #1) in Fig. 18(a) is characterized by AFM flow mark, commonly observed in the fully AFM finished surface [17,18], indicating that most of SLM generating irregular patterns (e.g., unmolten powder, local wavings, and pits) were completely removed. In the channel surface (type #1) after AFM in Fig. 18(a), its Rz value was measured to be 1.6 μm. Therefore, it can be said that the fully AFM finished SLM built channel surface can meet the conventional pipe's

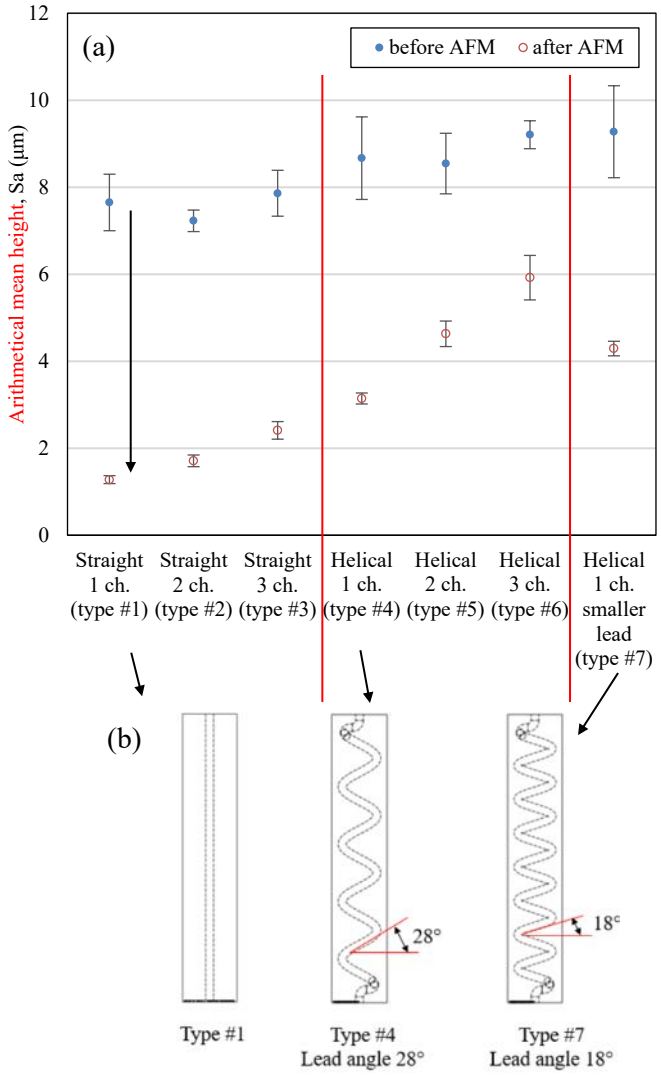

Fig. 20. (a) The areal roughness of the conformal cooling channel surfaces before and after AFM, (b) conformal channels (type #1, #4, #7) having a different lead angle.

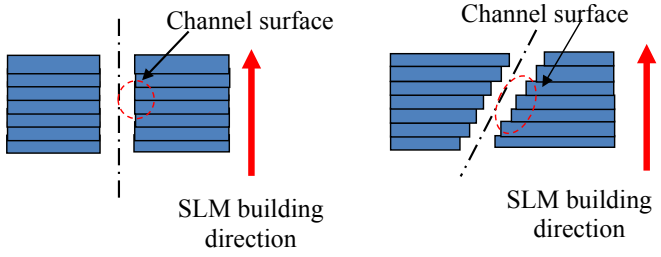

Fig. 21. Staircase effect observed on the inclined channel surface in SLM.

internal channel Rz values.

4. Conclusion

This paper aimed to investigate the efficiency of the AFM finishing process to decrease surface roughness in complex channels. Seven different geometries of single and multiple channels have been designed and built by SLM. Then, the internal cooling channel surfaces were finished with AFM, and their surfaces were analyzed in terms of areal parameters (ISO 25178-2).

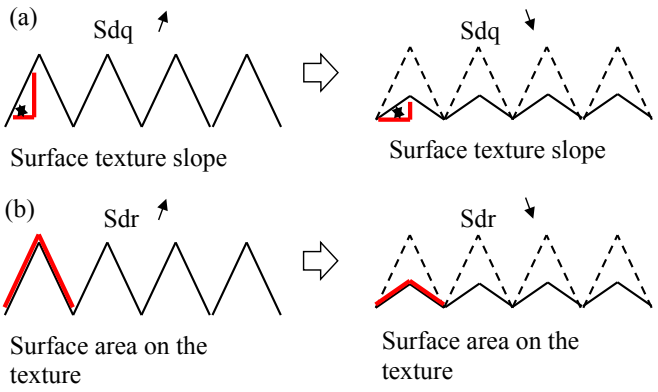

Fig. 22. Schematic illustration of the evolution: (a) Sdr and (b) Sdq values of the surface.

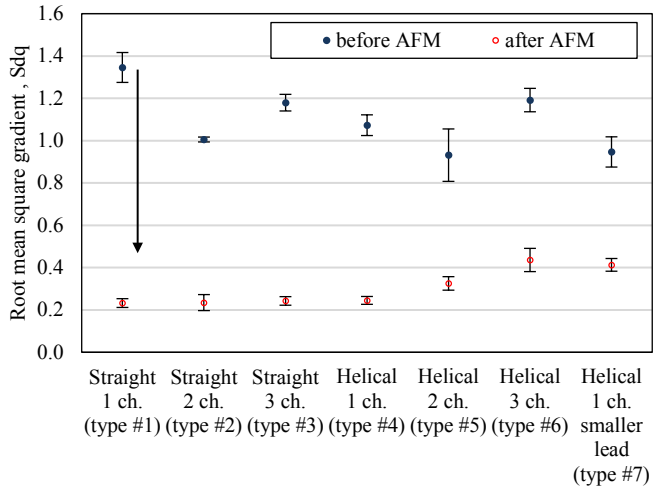

Fig. 23. The root mean square gradient, Sdq, of SLM internal channel surfaces before and after AFM.

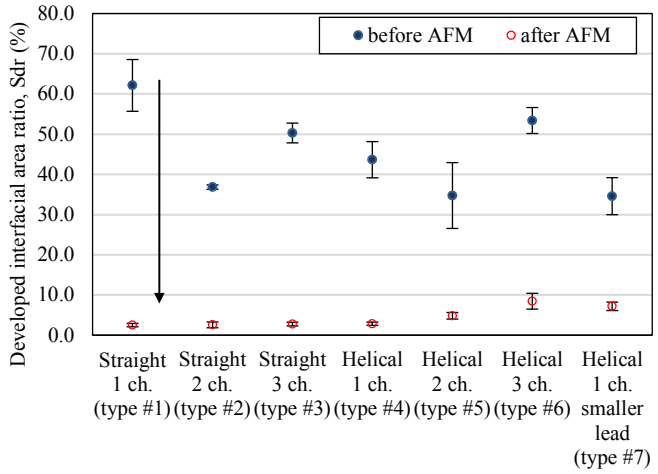

Fig. 24. The developed interfacial area ratio, Sdr, of the SLM internal channel surfaces before and after AFM.

- AFM is shown to be effective in improving all proposed types of SLM conformal cooling channels' arithmetical mean height, Sa. In particular, a straight conformal cooling channel surface (type #1) has improved from 7.6 to 1.3 μm Sa by AFM finishing.

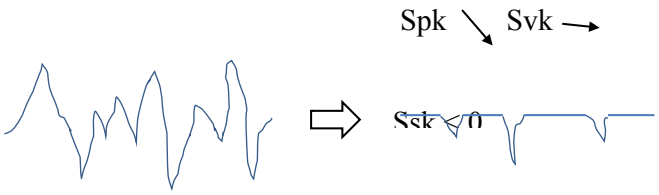

Fig. 25. Schematic illustration of surface topography and areal parameter evolution during AFM.

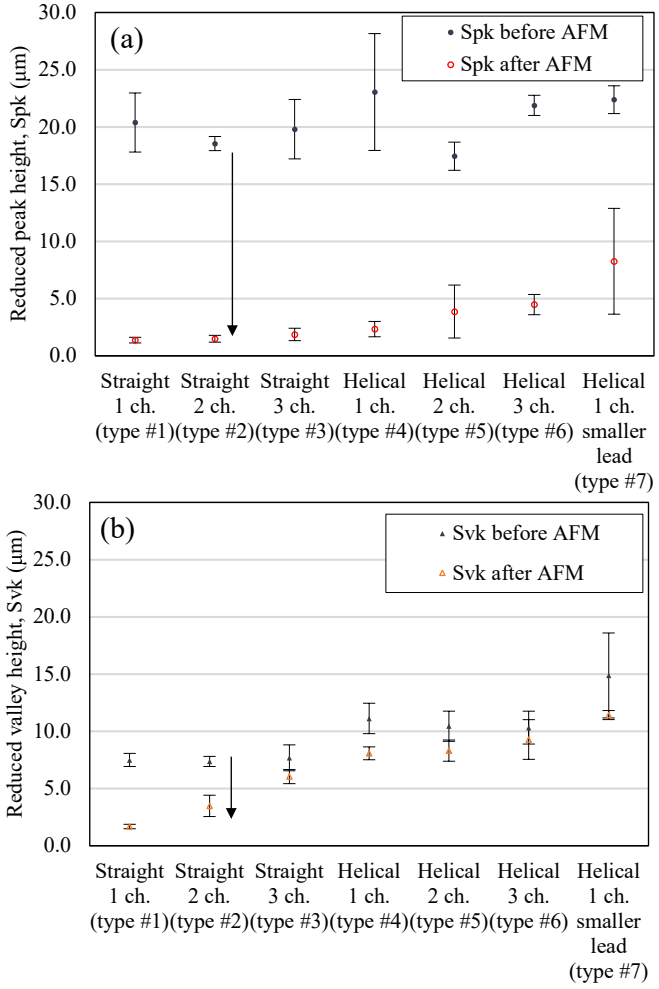

Fig. 26. (a) The reduced peak height, Spk, before and after AFM, (b) The reduced valley height, Svk, before and after AFM.

- The velocity of AFM media flow in the channels can affect the progress of the arithmetical mean height, Sa;
  - The more numbers of internal channels are present, the lower velocity of AFM media flow was observed. The velocities of AFM flow in two and three straight channels are 27% and 45% lower than that in one straight channel. The velocities of AFM flow in two and three helical channels are 47% and 66% lower than that in one helical channel. Thus, the progress of arithmetical mean height, Sa, in the multi-channel is lower than that in the single channel.
  - The longer the internal channel is, the lower velocity of AFM media flow was seen. The velocities of AFM flow in one helical channel with big and small lead angle are 26% and 46% lower than that in one straight channel. Thus, the progress of arithmetical mean height, Sa, in the longer channel is lower than that in the shorter channel.

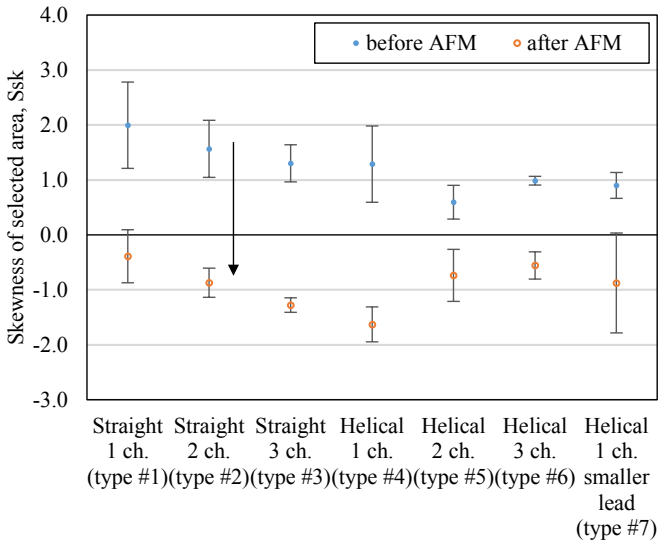

Fig. 27. The skewness of the selected area, Ssk.

- The amount of AFM media flowing through the channels also affects the reduction in the areal roughness, Sa;
  - Less amount of AFM media flows through the multi-channel than through the single channel.
  - Thus, it is necessary to increase the AFM media volume in the multi-channel to keep the same amount of AFM media flowing through the single channel.

Areal parameters on the internal cooling channel surfaces were also found to be sensitive to surface finish by AFM;

- Since the peak regions were removed by AFM, the developed interfacial area ratio, Sdr, and the root mean square gradient decreased significantly, indicating that rough surfaces become smooth ones.
- The initial SLM internal channel surface is characterized by much higher reduced peak value, Spk, than reduced valley one, Svk.
- After AFM, the high peak regions were removed by AFM, and the AFM flow lines and the remaining valley regions were visible. Thus, the Svk value on the internal cooling channel surface becomes higher than the Spk value after AFM. Consequently, its skewness, Ssk, changes from high positive to high negative values after AFM.

This study can provide more insights on the capability of the AFM process to finish the SLM built conformal cooling channel. Previous studies showed that cooling efficiency of the internal cooling channel increased with its surface roughness decreasing. Therefore, this study suggests that the AFM finished SLM built internal cooling channel can enhance its cooling efficiency as compared to the SLM as-built one. Also, in fully AFM finished SLM built internal channel, its surface roughness is shown to be comparable to that of the cooling pipes used in the conventional mold.

Declaration of competing interest

The authors declare that they have no known competing financial interests or personal relationships that could have appeared to influence the work reported in this paper.

The authors also thank:

- Extrude Hone® for providing the AFM machine and AFM media.
- Jean-Christophe BORNEAT to fabricate SLM specimens in IPC.
- Hervé SEUX and Patrick POLLY for AFM fixture manufacturing in ENISE.

Acknowledgements

The authors are grateful to I@L Carnot MELTED for the financial support of this research.

Nomenclature

l_{lead}	Lead length of a helical channel (mm)
θ	Lead angle of a helical channel (°)
$d_{channel}$	Channel diameter of an internal channel (mm)
d_r	Rotating diameter of a helical channel center (mm)
Sa	Arithmetical mean height of the scale limited surface (μm)
Sdr	Developed interfacial area ratio (%)
Sdq	Root mean square gradient ( )
Spk	Reduced peak height (μm)
Svk	Reduced valley height (μm)
Ssk	Skewness of selected area ( )

References

[1] Sachs E, Allen S, Cima M, Wylonis E, Guo H. Production of injection molding tooling with conformal cooling channels using the three dimensional printing process. Polym Eng Sci 2000;40:1232–47.
[2] Dimla DE, Camilotto M, Miani F. Design and optimization of conformal cooling channels in injection moulding tools. J Mater Process Technol 2005;164–165:1294–300.
[3] Park H, Dang X. Development of a smart plastic injection molds with conformal cooling channels. Procedia Manuf 2017;10:48–59.
[4] Armillotta A, Baraggi R, Fasoli S. SLM tooling for die casting with conformal cooling channels. Int J Adv Manuf Technol 2014;71:573–83.
[5] Townsend A, Senin N, Blunt L, Leach RK, Talyor JS. Surface texture metrology for metal additive manufacturing: a review. Precis Eng 2016;46:34–47.
[6] Tan KL, Yeo SH. Surface modification of additive manufactured components by ultrasonic cavitation abrasive finishing. Wear 2017;378–379:90–5.
[7] Marimuth S, Triantaphyllou A, Antar M, Wimpenny D, Morton H, Beard M. Laser polishing of selective laser melted components. Int J Mach Tool Manufact 2015;95:97–104.
[8] Lyczkowksa E, Szymczyk P, Bybala B, Chlebus E. Chemical polishing of scaffolds made of Ti-6Al-7Nb alloy by additive manufacturing. Arch. Civil Mech. Eng. 2014;14:586–94.
[9] Urlea V, Brailovsk V. Electropolishing and electropolishing-related allowances for powder bed selectively laser-melted Ti-6Al-4V alloy components. J Mater Process Technol 2017;242:1–11.
[10] Furumoto T, Ueda T, Amino T, Kusunoki D, Hosokawa A, Tanaka R. Finishing performance of cooling channel with face protuberance inside the molding die. J Mater Process Technol 2012;212:2154–60.
[11] Furumoto T, Ueda T, Amino T, Hosokawa A. A study of internal face finishing of the cooling channel in injection mold with free abrasive grains. J Mater Process Technol 2011;211:1742–8.
[12] Zhang J, Hu J, Wang H, Kumar AS, Chaudhari A. A novel magnetically driven polishing technique for internal surface finishing. Precis Eng 2018;54:222–32.
[13] Yamaguchi H, Shinmura T, Kobayshi A. Development of an internal magnetic abrasive finishing process for nonferromagnetic complex shaped tubes. JSME Int. J., Ser. C 2001;44:275–81.
[14] Williams RE, Walczyk DF, Dang HT. Using abrasive flow machining to seal and finish conformal channels in laminated tooling. Rapid Prototyp J 2007;13:64–75.
[15] Duval-Chaneac MS, Han S, Claudin C, Salvatore F, Rech J. Experimental study of finishing of internal laser melting (SLM) surface with abrasive flow machining (AFM). Precis Eng 2018;54:1–6.
[16] Jain RK, Jain VK, Dixit PM. Modeling of material removal and surface roughness in abrasive flow machining process. Int J Mach Tool Manufact 1999;39:1903–23.
[17] Jain VK, Adsul SG. Experimental investigation into abrasive flow machining (AFM). Int J Mach Tool Manufact 2000;40:1003–21.
[18] Loveless TR, Williams RE, Rajurkar KP. A study of the effects of abrasive-flow finishing on various machined surfaces. J Mater Process Technol 1994;47:133–51.
[19] Kumar S, Hiremath SS. A review on abrasive flow machining (AFM). RAEREST 2016;25:1297–304. Procedia Technol.
[20] Petare AC, Jain NK. A critical review of past research and advances in abrasive flow finishing process. Int J Adv Manuf Technol 2018;97:741–82.
[21] Liu C, Cai Z, Dai Y, Huang N, Xu F, Lao C. Experimental comparison of the flow rate and cooling performance of internal cooling channels fabricated via selective laser melting and conventional drilling process. Int J Adv Manuf Technol 2018;96:2757–67.
[22] Snyder JC. Improving turbine cooling through control of surface roughness in the additive manufacturing process. PhD thesis. The Pensylvania State University; 2019.
[23] Farshad FF, Rieke HH. Surface-Roughness design values for modern pipes. SPE Drill Complet 2016:212–5.
[24] Mazur M, Leary M, McMillan M, Elambasseril J, Brandt M. SLM additive manufacture of H13 tool steel with conformal cooling and structural lattices. Rapid Prototyp J 2016;22:504–18.